Supplementary Information to "Deep seafloor hydrothermal vent communities buried by volcanic ash from the 2022 Hunga eruption"

Roxanne A. Beinart[1†*], Shawn M. Arellano[2,3,4†], Marcus Chaknova[5,6,7], Jasper Meagher[1], Andrew J. Davies[1,8], Joseph Lopresti[1], Emily J. Cowell[9], Melissa Betters[9], Tanika M. Ladd[2], Caitlin Q. Plowman[5,6], Lauren N. Rice[5,6], Dexter Davis[2], Maia Heffernan[4], Vanessa Jimenez[1,2,3], Tessa Beaver[2,3], Johann Becker[10], Sebastien Bergen[5,6], Livia Brunner[11], Avery Calhoun[5,6], Michelle Hauer[1], Aubrey Taradash[5,6], Thomas Giachetti[7], Craig M. Young[5,6]

1 Graduate School of Oceanography, University of Rhode Island, Narragansett, USA
2 Shannon Point Marine Center, Western Washington University, Anacortes, USA
3 Biology Department, Western Washington University, Bellingham, USA
4 Marine and Coastal Science Program, Western Washington University, Bellingham, USA
5 Oregon Institute of Marine Biology, University of Oregon, Charleston, USA
6 Department of Biology, University of Oregon, Eugene, USA
7 Department of Earth Sciences, University of Oregon, Eugene, USA
8 Department of Biological Sciences, University of Rhode Island, Kingston, USA
9 Department of Biology, Temple University, Philadelphia, USA
10 Department of Ocean Engineering, University of Rhode Island, Narragansett, USA
11 Department of Ocean Systems, Royal Netherlands Institute for Sea Research, Texel, Netherlands

† Contributed equally
* Correspondence to rbeinart@uri.edu

Supplementary Tables

Table S1: Dives sites, coordinates, associated ROV Jason dive numbers, and total dive time lengths at each vent field.

Vent field	Lat	Lon	Dive Numbers	Total Dive Duration (hours)
Kilo Moana	-20.083269	-176.16671	J2-1402, -1409, -1410	30.93
Tow Cam	-20.319979	-176.14002	J2-1403, -1412	34.8
Tahi Moana	-20.681211	-176.18286	J2-1404, 1413	42.15
ABE	-20.762134	-176.19093	J2-1405, 1406, 1414	52.22
Tu'i Malila	-21.99036	-176.57007	J2-1407, -1415	33.78
Mariner	-22.179786	-176.60257	J2-1408	14.37

Table S2: Ash thickness data. In some cases, triplicate measurements were taken when ROV was in a single location, 1-2 meters apart.

Dive	Vent field	Lat	Lon	Depth (m)	Ash Thickness (cm)
J2-1404	THM	-20.6820577	-176.18329	2234	8
J2-1404	THM	-20.6821264	-176.1833103	2234	6
J2-1404	THM	-20.6821372	-176.1838656	2240	19
J2-1404	THM	-20.6821395	-176.1838615	2240	11
J2-1405	ABE	-20.7619159	-176.1916454	2133	17, 15, 10
J2-1405	ABE	-20.7647803	-176.1925047	2134	15
J2-1405	ABE	-20.7647769	-176.1925026	2134	18
J2-1405	ABE	-20.7647779	-176.1924937	2134	15
J2-1405	ABE	-20.7652683	-176.1924937	2136	15
J2-1409	KM	-22.0532208	-176.1332964	2624	23, 23, 18
J2-1410	KM	-20.0536658	-176.1322012	2630	53
J2-1412	TC	-20.137332	-176.13647	2696	64
J2-1412	TC	-20.317354	-176.13651	2696	80
J2-1412	TC	-20.3169801	-176.1362283	2696	150
J2-1412	TC	-20.3178769	-176.1372119	2723	53
J2-1413	THM	-20.6823016	-176.1821561	2240	15
J2-1413	THM	-20.6823095	-176.1821501	2240	11
J2-1413	THM	-20.6823185	-176.1821603	2239	15
J2-1414	ABE	-20.76185	-176.19168	2132	15
J2-1414	ABE	-20.765277	-176.19226	2136	11, 8, 8
J2-1414	ABE	-20.765275	-176.19228	2136	11
J2-1414	ABE	-20.765245	-176.19234	2135	15

Table S3: Vent field, dive number, timestamp, and location of canvas bag collections of ash

Vent field	Dive	Timestamp	Lat	Lon	Depth (m)
Kilo Moana	J2-1410	2022-04-19T02:30:27.004Z	-20.053656	-176.1322	2630.222
Tow Cam	J2-1403	2022-04-05T13:41:01.332Z	-20.316239	-176.13638	2727.213
Tow Cam	J2-1412	2022-04-20T23:15:01.643Z	-20.317836	-176.13718	2723.39
Tahi Moana	J2-1404	2022-04-08T04:37:41.647Z	-20.682124	-176.18385	2240.212
Tahi Moana	J2-1413	2022-04-22T06:31:53.756Z	-20.682179	-176.1825	2234.208
ABE	J2-1406	2022-04-12T05:47:55.112Z	-20.766029	-176.19203	2151.127
ABE	J2-1414	2022-04-24T03:46:42.485Z	-20.765213	-176.19234	2134.936

Table S4: Metadata for each ROV dive from the 2019 and 2022 expeditions including total dive duration and the total number of images analyzed for quantitative comparison before and after the eruption.

Site	Vehicle	Dive ID	Launch lat (ddeg)	Launch lon (ddeg)	Date	Duration (hours)	Total Images Analyzed	Total Images Classifiable
Tow Cam	Victor 6000	721	-20.317833	-176.13733	31/03/19	41.1	686	345
	Victor 6000	723	-20.317833	-176.13733	05/04/19	30.4	197	100
	Victor 6000	730	-20.317833	-176.13733	25/04/19	7.27	948	404
	Jason II	J2-1403	-20.319979	-176.14002	05/04/22	20.1	581	274
	Jason II	J2-1412	-20.320352	-176.13686	20/04/22	14.7	164	65
ABE	Victor 6000	731	-20.763333	-176.19133	26/04/19	21.9	1094	346
	Jason II	J2-1405	-20.762134	-176.19093	09/04/22	22.8	374	151
	Jason II	J2-1406	-20.762049	-176.19225	12/04/22	6.6	393	55
	Jason II	J2-1414	-20.761006	-176.19141	23/04/22	22.8	336	158
Tu'i Malila	Victor 6000	722	-21.988000	-176.56800	03/04/19	60.9	2044	1008
	Jason II	J2-1407	-21.990360	-176.57007	12/04/22	24.9	974	312
	Jason II	J2-1415	-21.988849	-176.56807	26/04/22	8.93	53	40

Table S5: Organisms assessed for abundance, including their SACFOR size class, category for analysis, and mean size as estimated through organismal collections in 2022, as available, and/or published literature.

SACFOR Size class	Organismal Category	Included Taxa	Size (cm) for field of view scaling
Chemosymbiotic			
3-15	*Alviniconcha*[a]	*Alviniconcha boucheti, Alviniconcha strummeri, Alviniconcha kojimai*	5.1[b]
3-15	*Ifremeria*[a]	*Ifremeria nautilei*	4.9[c]
3-15	*Bathymodiolus*[a]	*Bathymodiolus septemdierum*	8.6[d]
Heterotrophic			
1-3	Alvinellid worms	*Paralvinella fijiensis*, *Paralvinella unidentata*	1.8[1e]
1-3	Anemones (small)	*Actinostolidae* sp.; *Amphianthus* sp.	2.5[2,3f]
3-15	Anemones (large)	*Pacmanactis hashimotoi*; *Cyananthea hourdezi*; *Alvinactis chessi*; *Chondrophellia orangina*; *Sagartiogeton erythraios*	12.5[2,3f]
1-3	Barnacles	*Vulcanolepas parensis*, *Balanomorpha* sp.	1.85[3–5g]
1-3	True crabs[a]	*Austinograea alayseae, Austinograea williamsi, Austinograea hourdezi, Austinograea jolliveti, Paralomis hirtella*	width 2.7[6–8h], length 3.2[6–8h]
1-3	Scale worms	*Branchinotogluma trifurcus, Thermopolynoe branchiata*	1.35[3i]
3-15	Shrimp (*Alvinocaris*)[a]	*Alvinocaris komaii*	5[9,10g]
1-3	Shrimp (*Rimicaris*)[a]	*Rimicaris vandoverae*	1.4[9,10i]
1-3	Squat lobsters[a]	*Munidopsis lauensis, Munidopsis starmer*	width 1.0[11,12j], length 1.3[11,12j]
3-15	Whelk	*Enigmaticolus desbruyesi*	6.2[13]
1-3	Zoanthids	Zoanthidea sp.	1.5[2f]

[a] Organismal groups used in field of view estimations. [b] Mean of organism widths calculated from collections taken in 2022, n = 297. [c] Mean of organism widths calculated from collections taken in 2022, n = 566. [d] Mean of organism lengths calculated from collections taken in 2022, n = 277. [e] total body length [f] the main pedal disk diameter excluding tentacle length. [g] pedunculum size, [h] Means of carapace width or length calculated from collections taken in 2022, n = 12. [i] Means of carapace width or length calculated from collections taken in 2022, n = 6 [j] Means of carapace width or length calculated from collections taken in 2022, n = 6

Table S6: SACFOR abundance scales used for organism counts in this study. The SACFOR abbreviations are: Superabundant, Abundant, Common, Frequent, Occasional and Rare.

	Organism Count		SACFOR scale for each organismal size group		
Field of view area (m^2)	Ind. m^{-2} **lower range**	**Ind. m^{-2} high range**	**1-3 cm**	**3-15 cm**	**>15 cm**
0.01	100	900	S		
0.1	10	90	A	S	
1	1	9	C	A	S
10	0.1	0.9	F	C	A
100	0.01	0.09	O	F	C
1000	0.001	0.009	R	O	F
10000	0.0001	0.0009		R	O
100000	0.00001	0.00009			R

Supplementary Figures

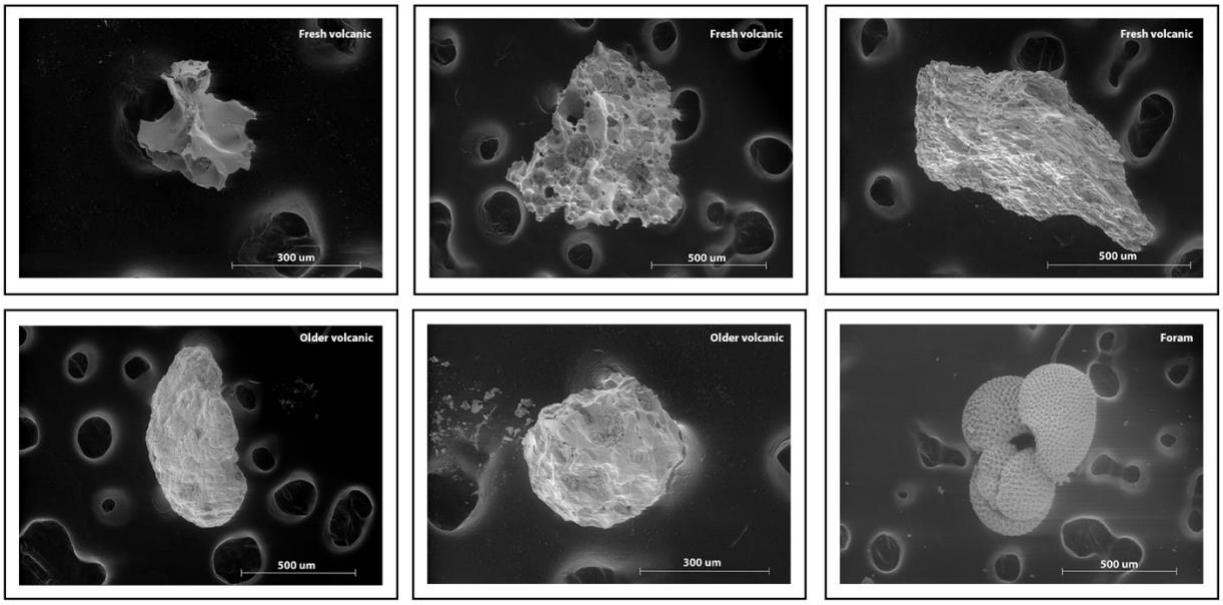

Fig.S1: Scanning electron micrographs of hand-picked particles from various vent fields. Particle categories identified in componentry analysis are fresh volcanic, older volcanic, and foraminifera. Top left) Fresh vesicular shard with fractured bubble walls; Top middle) Micro vesicular pumice; Top right) Elongated tubular pumice; Bottom left & bottom middle) Older volcanics with weathered surfaces; Bottom right) Common planktonic foraminifera found at all sites.

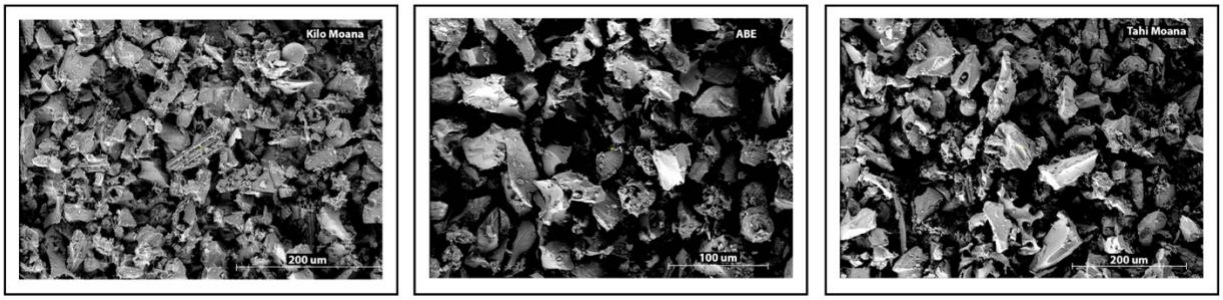

Fig.S2: Scanning electron micrographs of bulk ash sample from different vent fields. Left) Kilo Moana; Middle) ABE; Right) Tahi Moana.

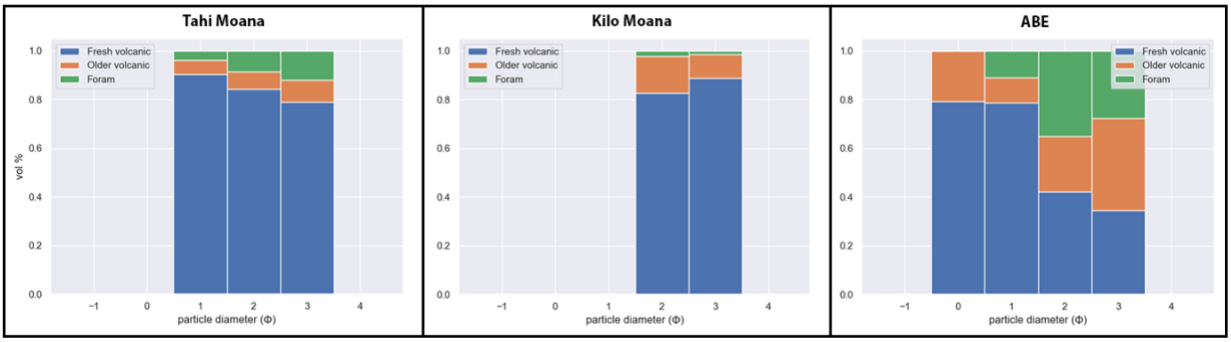

Fig.S3: Componentry from multiple vent fields. Left) Tahi Moana; Middle) Kilo Moana; Right) ABE. Y-axis represented in volume percent, x-axis represented in phi of the particle diameter.

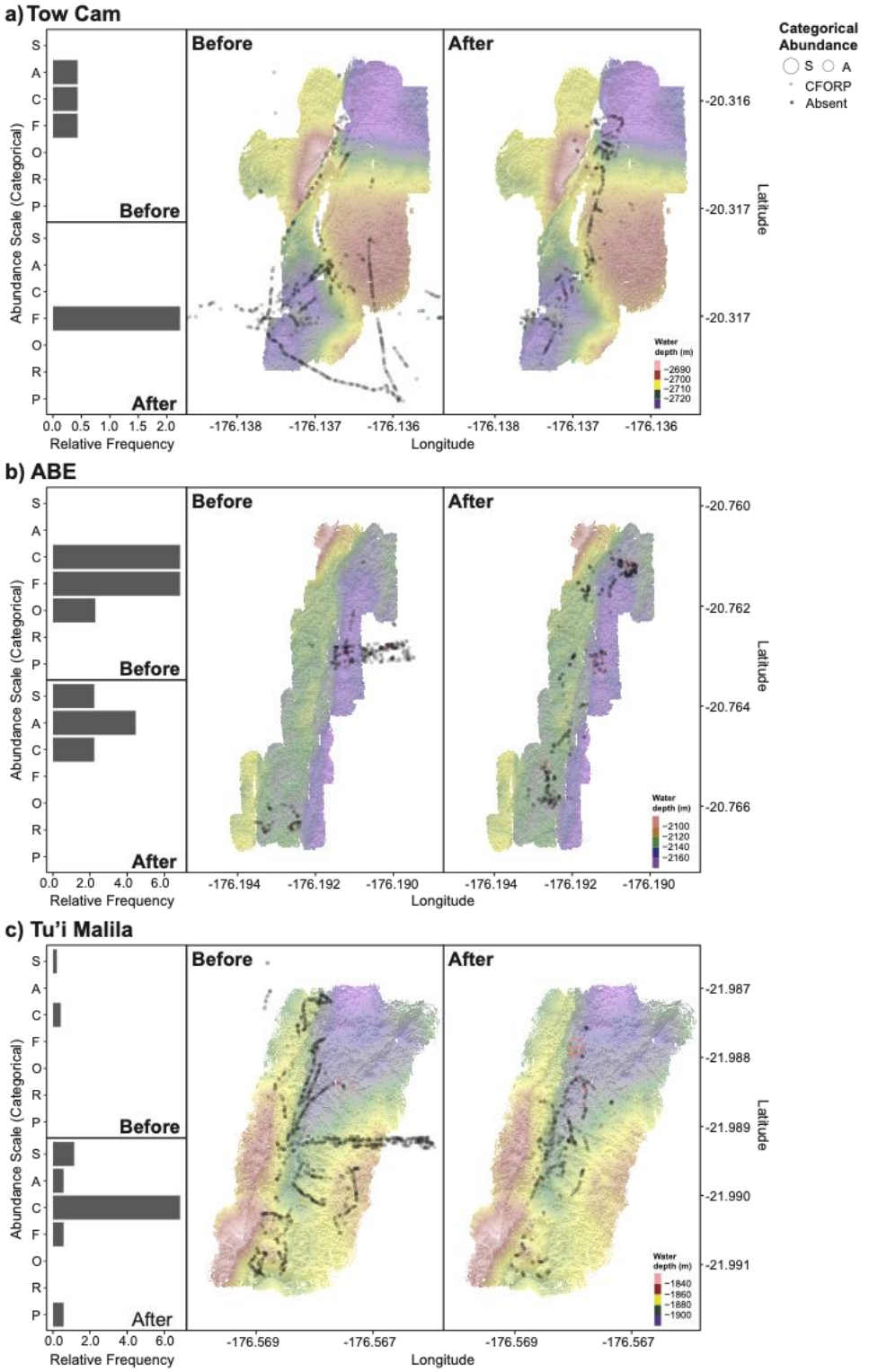

Fig.S4: Categorical abundances of alvinellid worms at a) Tow Cam, b) ABE, and c) Tu'i Malila vent fields before the Hunga volcanic eruption (2019) and after (2022). The categories Superabundant and Abundant are shown as differently sized red open circles, while Common, Frequent, Occasional, Rare, and Present are all shown as an open smaller red circle. Filled gray circles represent when the species was absent. Bathymetric data used to generate this figure was collected on the 2016 R/V Falkor (Schmidt Ocean Institute) cruise FK160407 and is publicly available through the Marine Geoscience Data System [14].

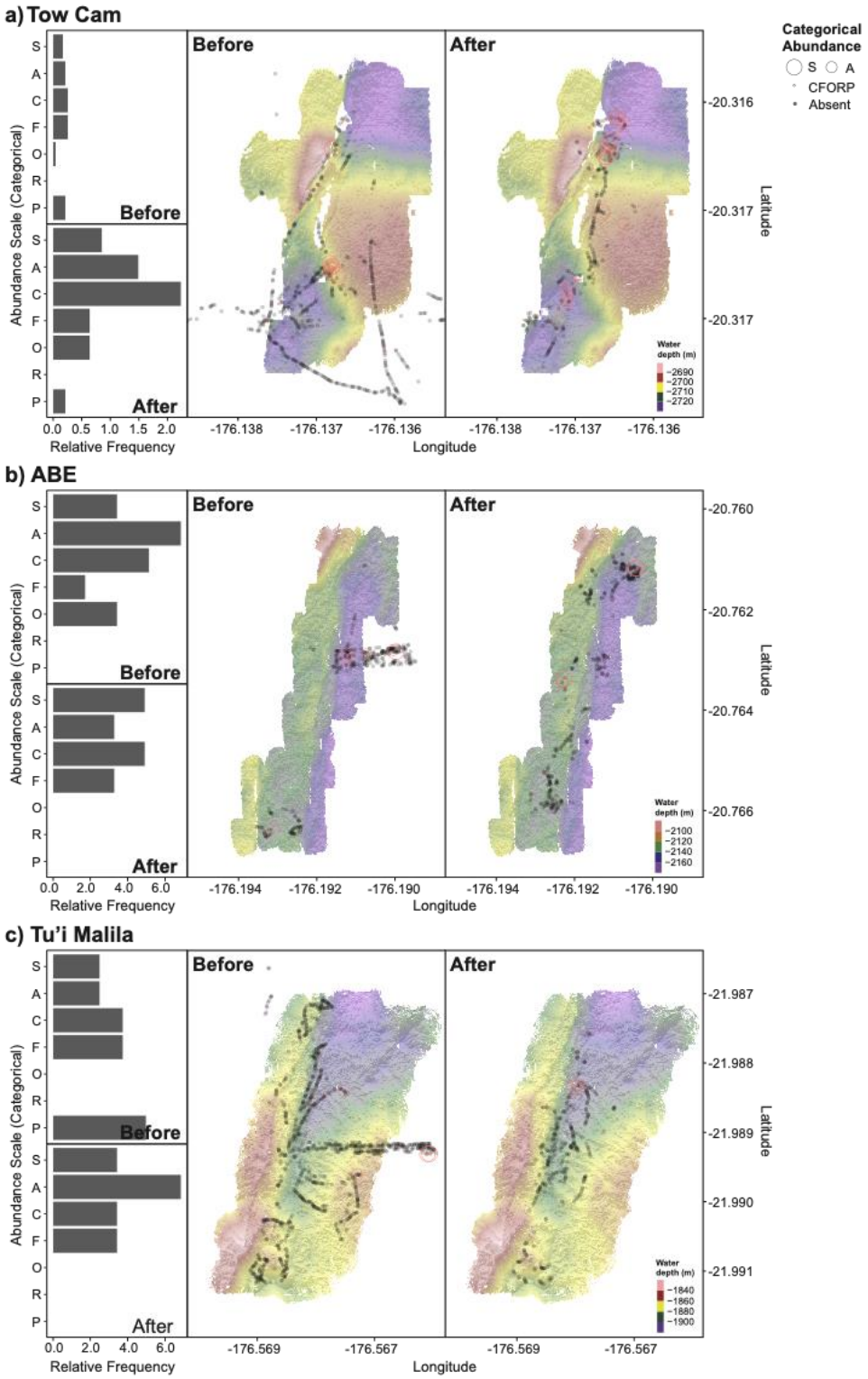

Fig.S5: Categorical abundances of large anemones at a) Tow Cam, b) ABE, and c) Tu'i Malila vent fields before the Hunga volcanic eruption (2019) and after (2022). The categories Superabundant and Abundant are shown as differently sized red open circles, while Common, Frequent, Occasional, Rare, and Present are all shown as an open smaller red circle. Filled gray circles represent when the species was absent. Bathymetric data used to generate this figure was collected on the 2016 R/V Falkor (Schmidt Ocean Institute) cruise FK160407 and is publicly available through the Marine Geoscience Data System [14].

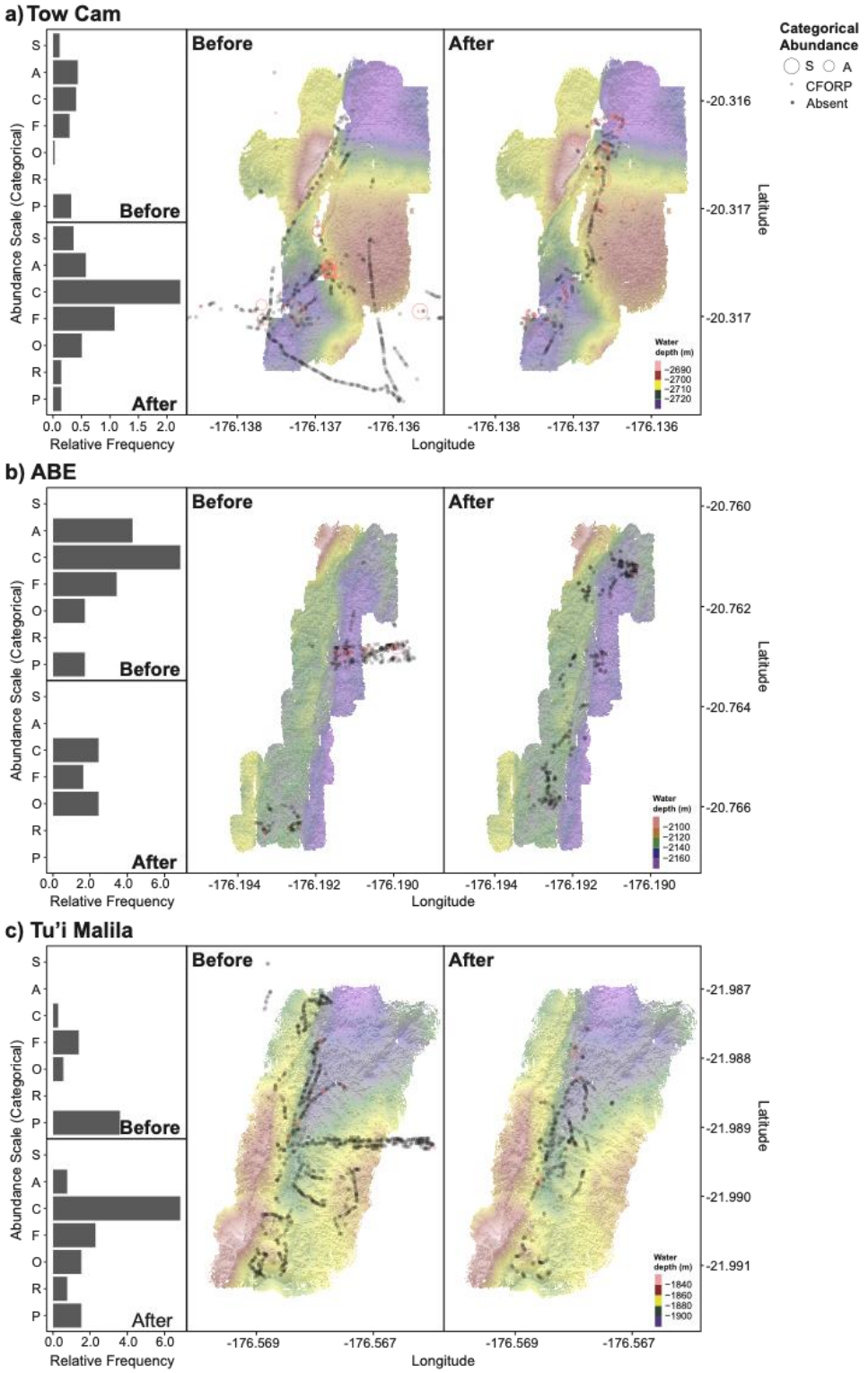

Fig.S6: Categorical abundances of small anemones at a) Tow Cam, b) ABE, and c) Tu'i Malila vent fields before the Hunga volcanic eruption (2019) and after (2022). The categories Superabundant and Abundant are shown as differently sized red open circles, while Common, Frequent, Occasional, Rare, and Present are all shown as an open smaller red circle. Filled gray circles represent when the species was absent. Bathymetric data used to generate this figure was collected on the 2016 R/V Falkor (Schmidt Ocean Institute) cruise FK160407 and is publicly available through the Marine Geoscience Data System [14].

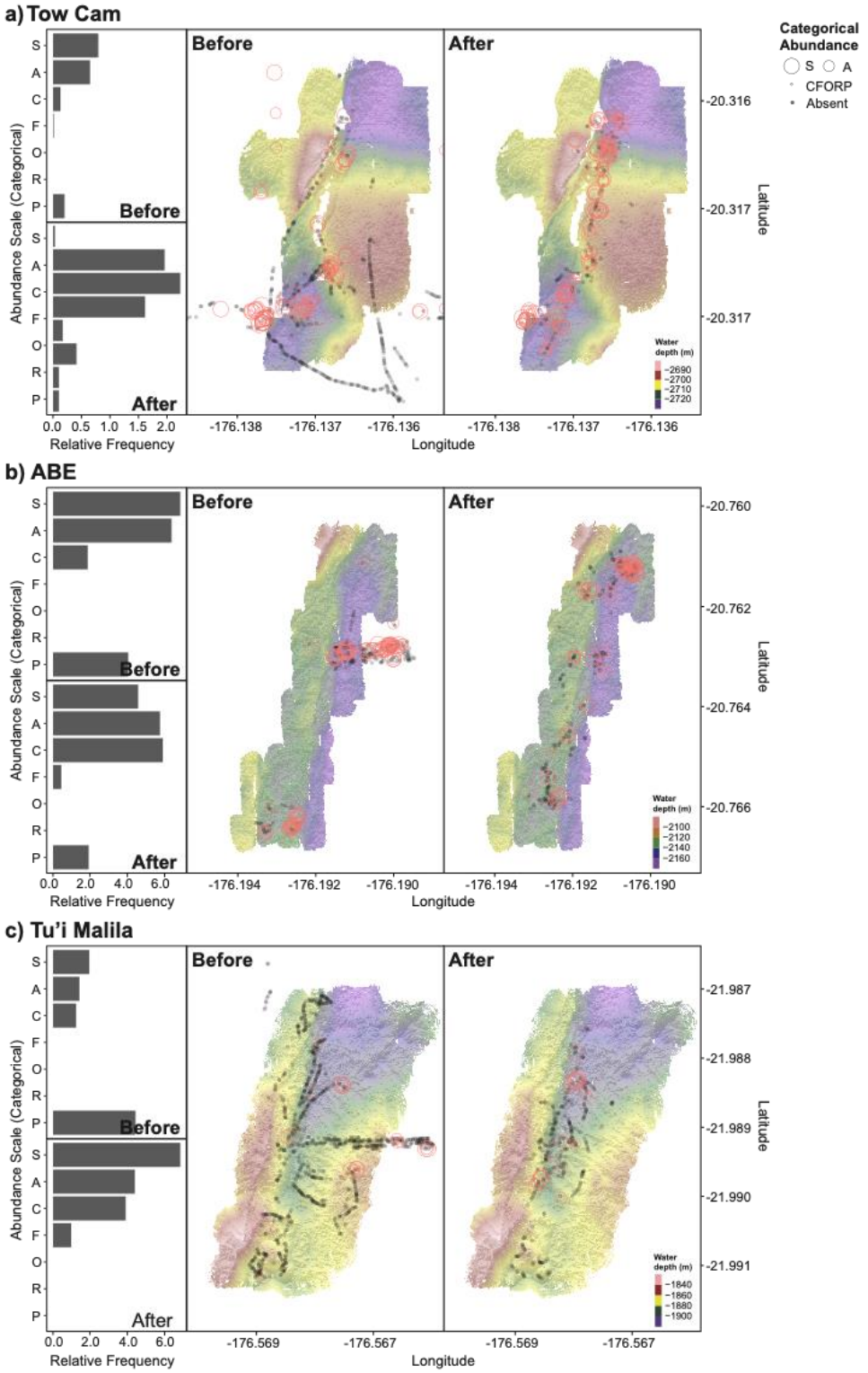

Fig.S7: Categorical abundances of barnacles at a) Tow Cam, b) ABE, and c) Tu'i Malila vent fields before the Hunga volcanic eruption (2019) and after (2022). The categories Superabundant and Abundant are shown as differently sized red open circles, while Common, Frequent, Occasional, Rare, and Present are all shown as an open smaller red circle. Filled gray circles represent when the species was absent. Bathymetric data used to generate this figure was collected on the 2016 R/V Falkor (Schmidt Ocean Institute) cruise FK160407 and is publicly available through the Marine Geoscience Data System [14].

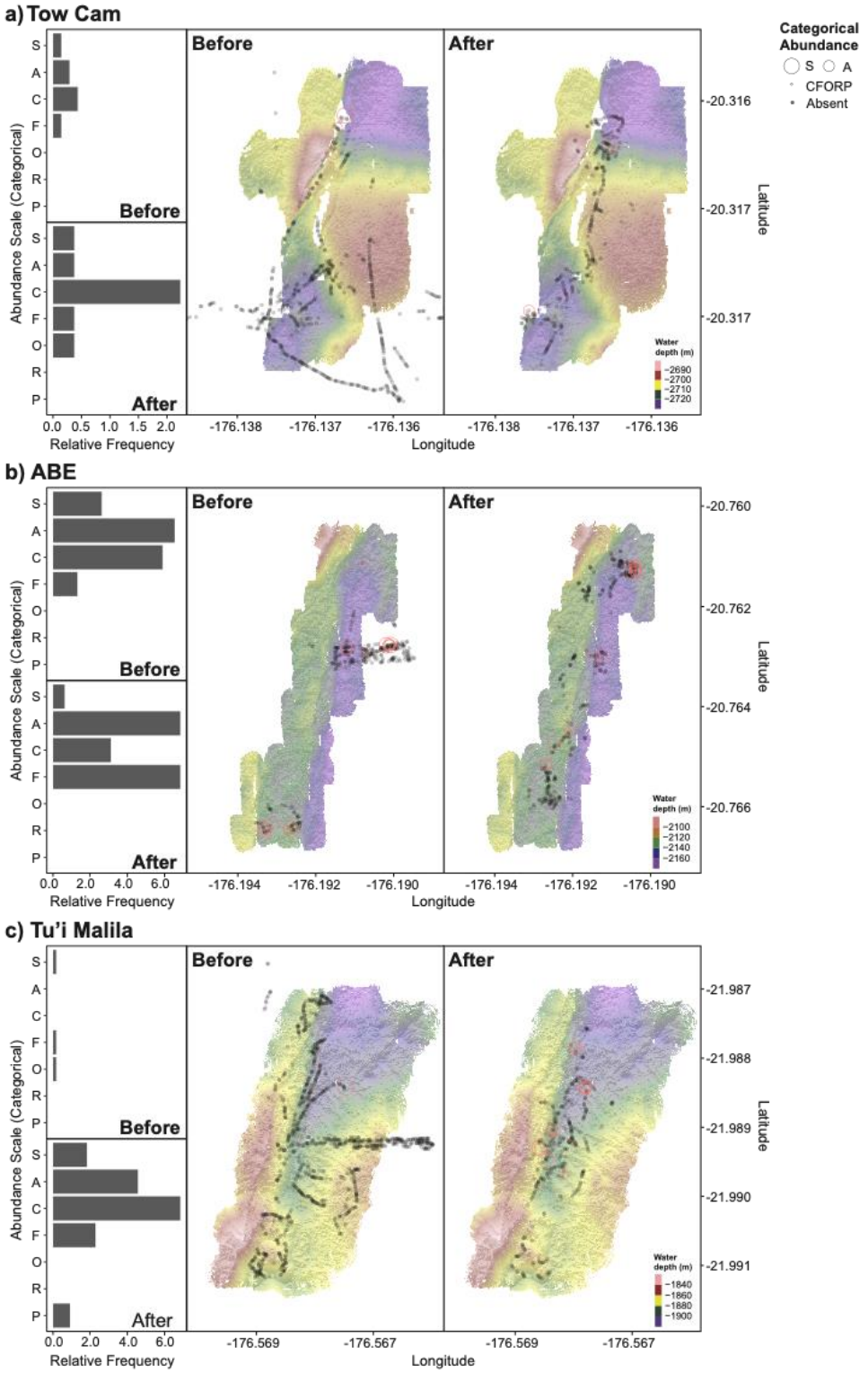

Fig.S8: Categorical abundances of scale worms at a) Tow Cam, b) ABE, and c) Tu'i Malila vent fields before the Hunga volcanic eruption (2019) and after (2022). The categories Superabundant and Abundant are shown as differently sized red open circles, while Common, Frequent, Occasional, Rare, and Present are all shown as an open smaller red circle. Filled gray circles represent when the species was absent. Bathymetric data used to generate this figure was collected on the 2016 R/V Falkor (Schmidt Ocean Institute) cruise FK160407 and is publicly available through the Marine Geoscience Data System [14].

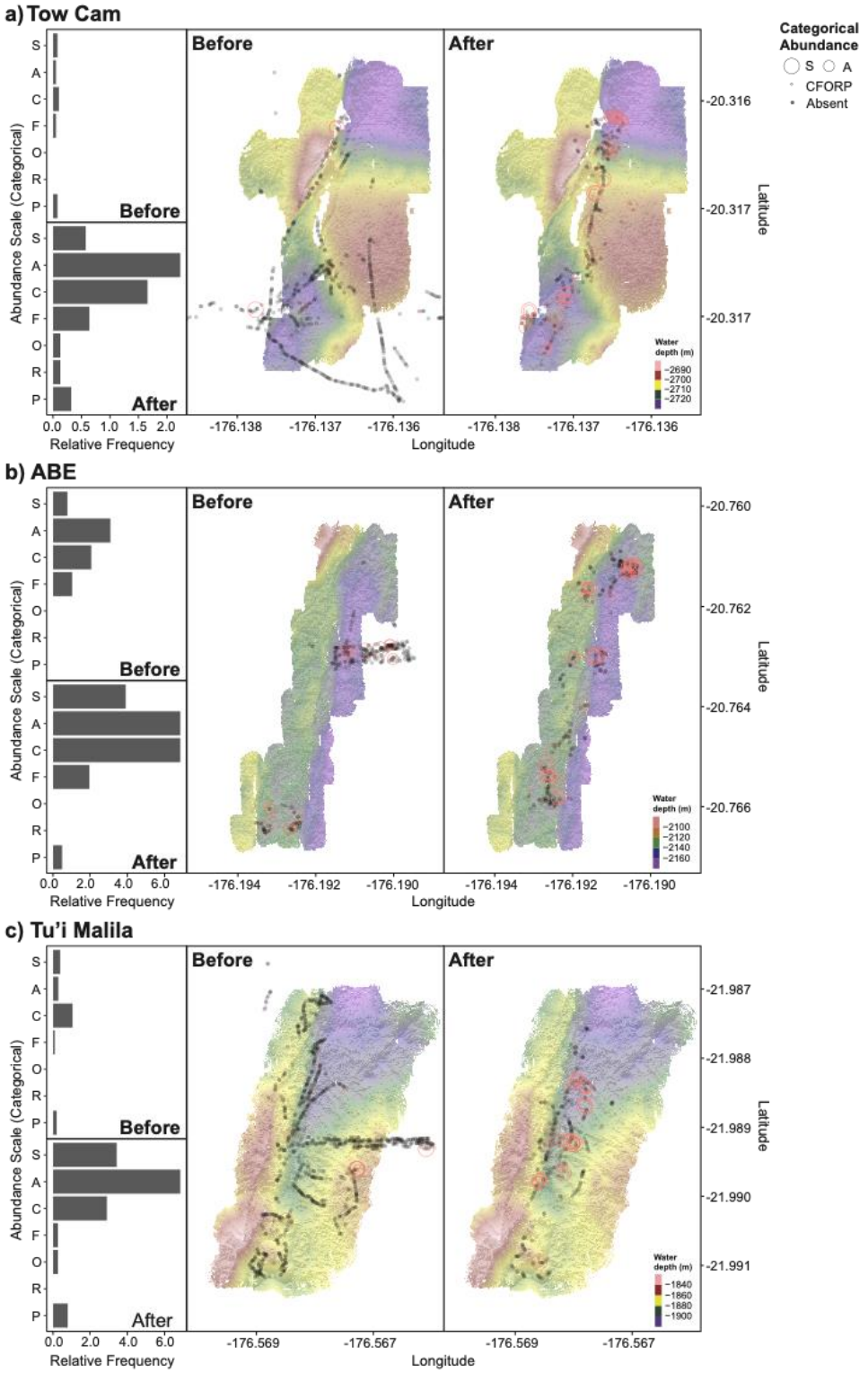

Fig.S9: Categorical abundances of *Alvinocaris* shrimp at a) Tow Cam, b) ABE, and c) Tu'i Malila vent fields before the Hunga volcanic eruption (2019) and after (2022). The categories Superabundant and Abundant are shown as differently sized red open circles, while Common, Frequent, Occasional, Rare, and Present are all shown as an open smaller red circle. Filled gray circles represent when the species was absent. Bathymetric data used to generate this figure was collected on the 2016 R/V Falkor (Schmidt Ocean Institute) cruise FK160407 and is publicly available through the Marine Geoscience Data System [14].

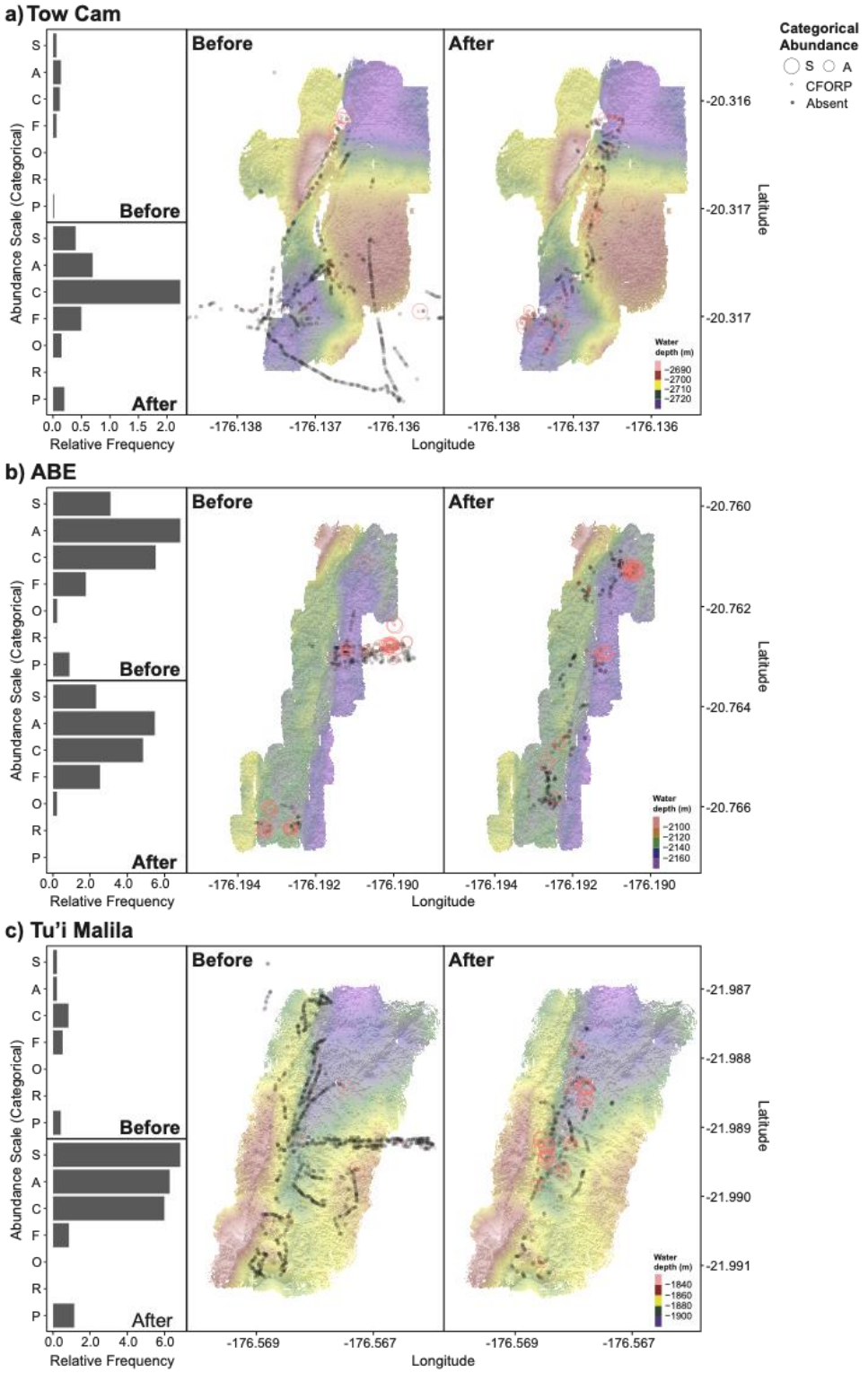

Fig.S10: Categorical abundances of *Rimicaris* shrimp at a) Tow Cam, b) ABE, and c) Tu'i Malila vent fields before the Hunga volcanic eruption (2019) and after (2022). The categories Superabundant and Abundant are shown as differently sized red open circles, while Common, Frequent, Occasional, Rare, and Present are all shown as an open smaller red circle. Filled gray circles represent when the species was absent. Bathymetric data used to generate this figure was collected on the 2016 R/V Falkor (Schmidt Ocean Institute) cruise FK160407 and is publicly available through the Marine Geoscience Data System [14].

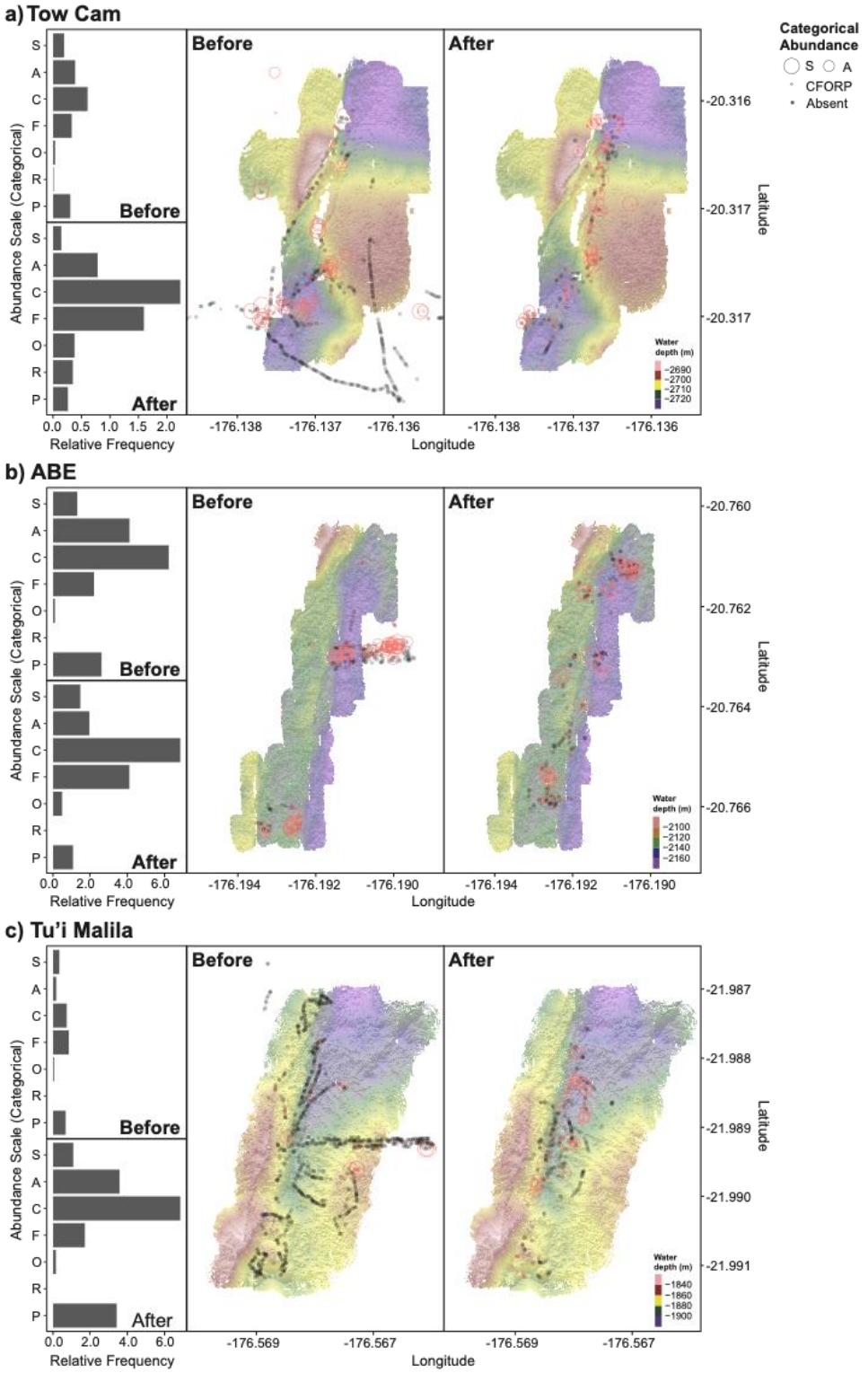

Fig.S11: Categorical abundances of squat lobsters at a) Tow Cam, b) ABE, and c) Tu'i Malila vent fields before the Hunga volcanic eruption (2019) and after (2022). The categories Superabundant and Abundant are shown as differently sized red open circles, while Common, Frequent, Occasional, Rare, and Present are all shown as an open smaller red circle. Filled gray circles represent when the species was absent. Bathymetric data used to generate this figure was collected on the 2016 R/V Falkor (Schmidt Ocean Institute) cruise FK160407 and is publicly available through the Marine Geoscience Data System [14].

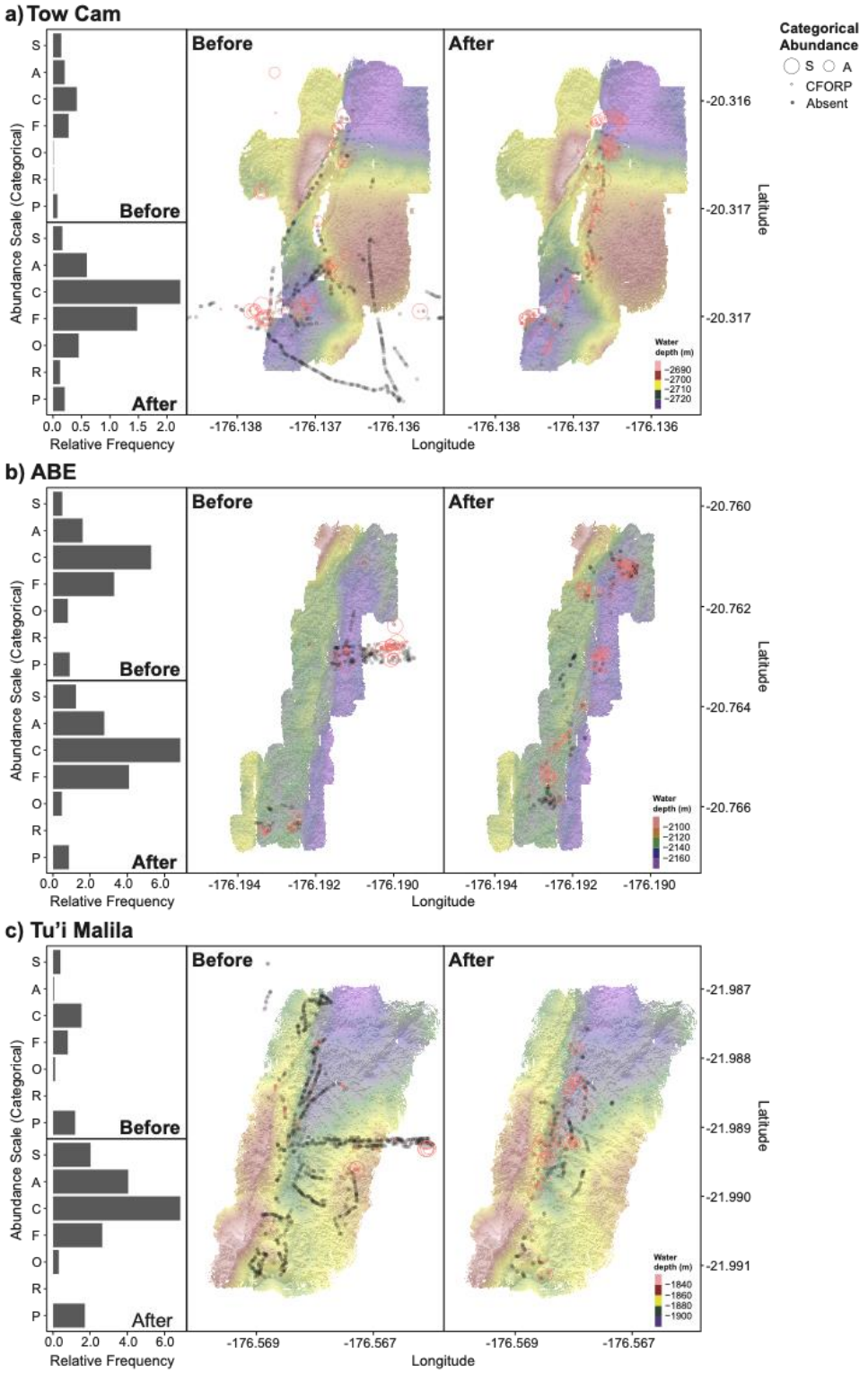

Fig.S12: Categorical abundances of true crabs at a) Tow Cam, b) ABE, and c) Tu'i Malila vent fields before the Hunga volcanic eruption (2019) and after (2022). The categories Superabundant and Abundant are shown as differently sized red open circles, while Common, Frequent, Occasional, Rare, and Present are all shown as an open smaller red circle. Filled gray circles represent when the species was absent. Bathymetric data used to generate this figure was collected on the 2016 R/V Falkor (Schmidt Ocean Institute) cruise FK160407 and is publicly available through the Marine Geoscience Data System [14].

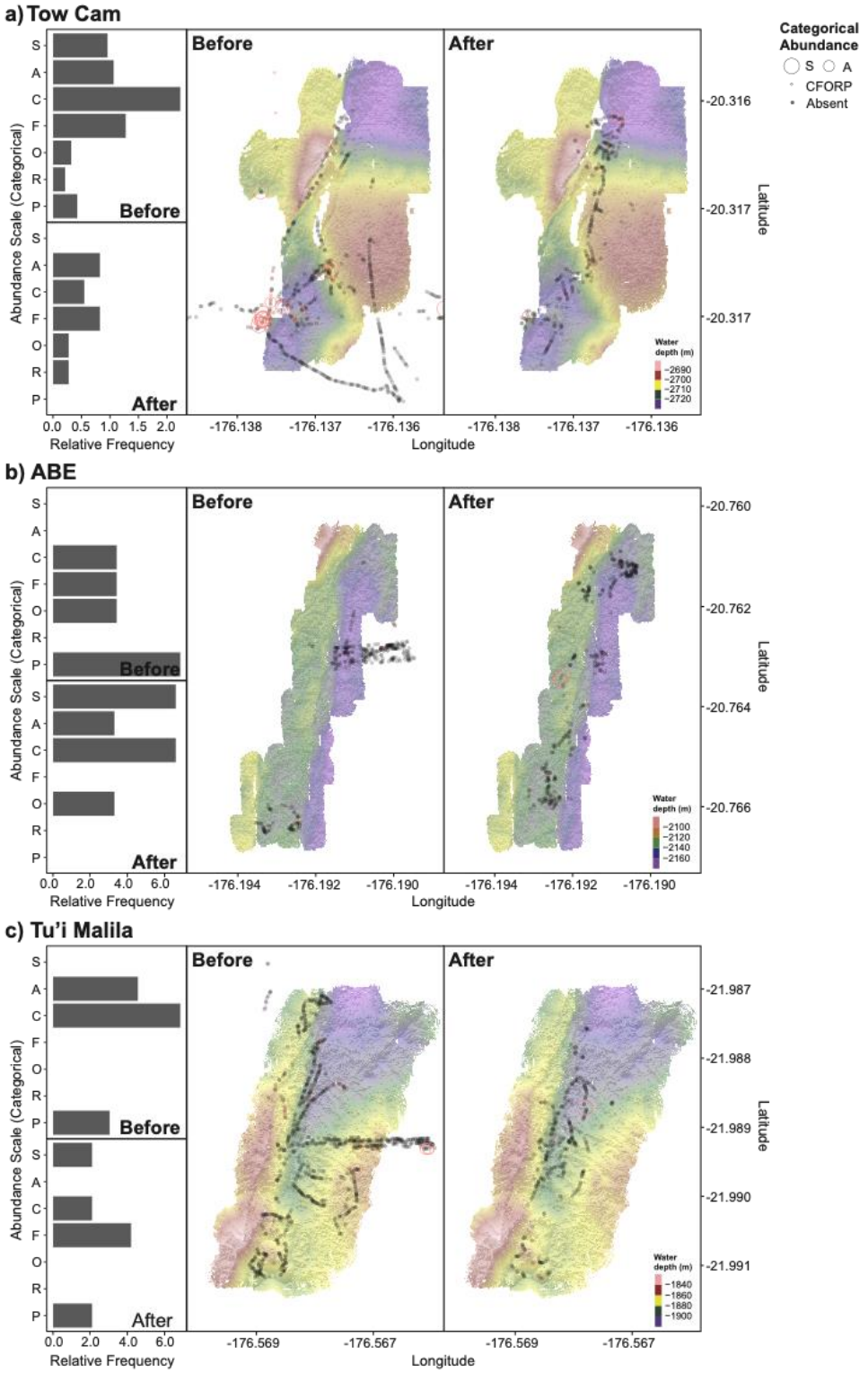

Fig.S13: Categorical abundances of whelks at a) Tow Cam, b) ABE, and c) Tu'i Malila vent fields before the Hunga volcanic eruption (2019) and after (2022). The categories Superabundant and Abundant are shown as differently sized red open circles, while Common, Frequent, Occasional, Rare, and Present are all shown as an open smaller red circle. Filled gray circles represent when the species was absent. Bathymetric data used to generate this figure was collected on the 2016 R/V Falkor (Schmidt Ocean Institute) cruise FK160407 and is publicly available through the Marine Geoscience Data System [14].

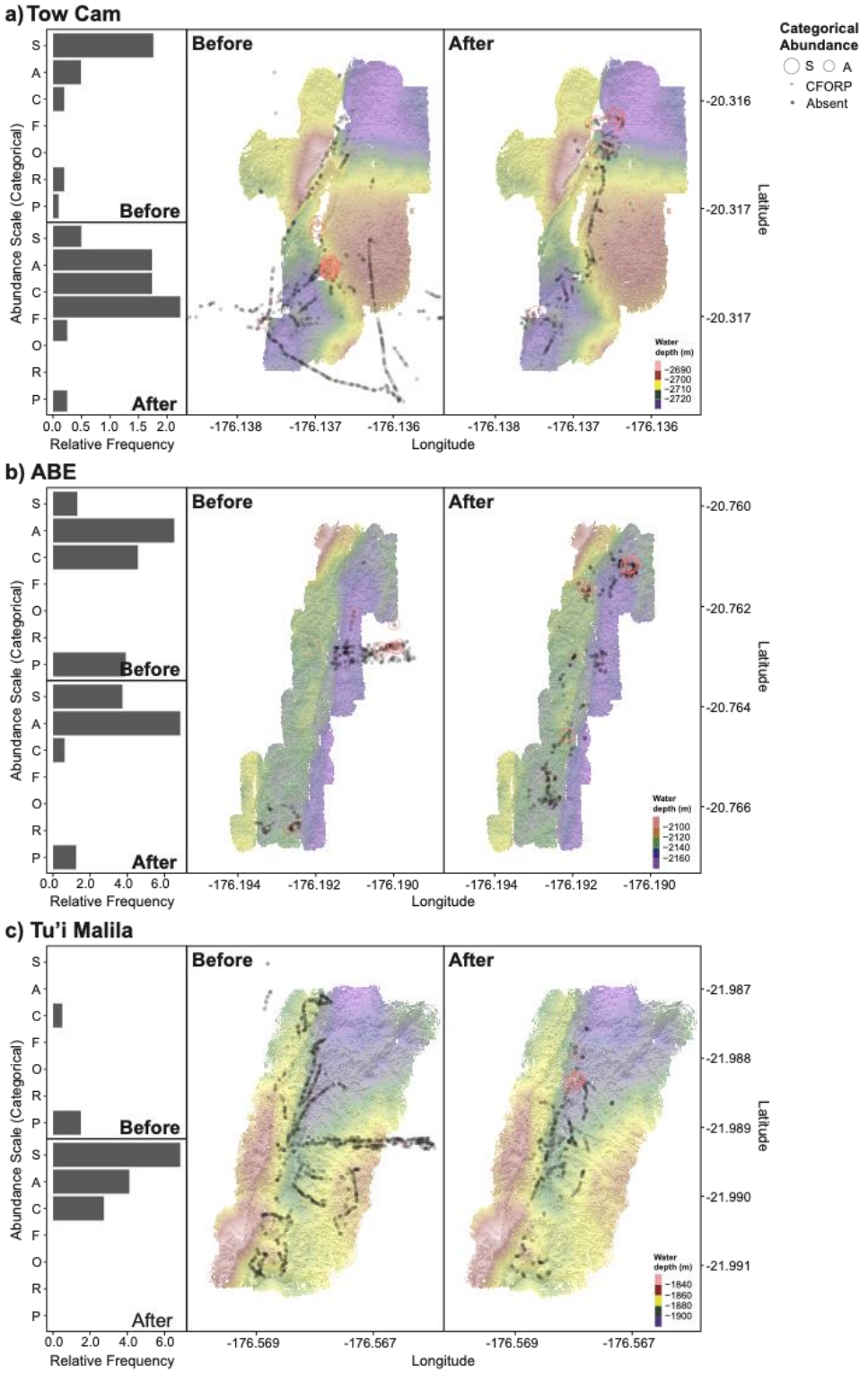

Fig.S14: Categorical abundances of zoanthids at a) Tow Cam, b) ABE, and c) Tu'i Malila vent fields before the Hunga volcanic eruption (2019) and after (2022). The categories Superabundant and Abundant are shown as differently sized red open circles, while Common, Frequent, Occasional, Rare, and Present are all shown as an open smaller red circle. Filled gray circles represent when the species was absent. Bathymetric data used to generate this figure was collected on the 2016 R/V Falkor (Schmidt Ocean Institute) cruise FK160407 and is publicly available through the Marine Geoscience Data System [14].

Supplementary References

1. Desbruyères, D. & Laubier, L. New species of Alvinellidae (Polychaeta) from the North Fiji back-arc basin hydrothermal vents (southwestern Pacific). *Proceedings of the Biological Society of Washington* **106**, 225–236 (1993).
2. Zelnio, K. a., Rodriguez, E. & Daly, M. Hexacorals (Anthozoa: Actiniaria, Zoanthidea) from hydrothermal vents in the south-western Pacific. *Marine Biology Research* **5**, 547–571 (2009).
3. Desbruyères, D., Hashimoto, J. & Fabri, M. C. Composition and biogeography of hydrothermal vent communities in western pacific back-arc basins. in *Geophysical Monograph Series* vol. 166 215–234 (2006).
4. Southward, A. J. Systematics and ecology of a new species of stalked barnacle (Cirripedia: Thoracica: Scalpellomorpha: Eolepadidae: Neolepadini) from the Pacific-Antarctic Ridge at 38 S. *Senckenbergiana maritima* **35**, 147–156 (2005).
5. Yamaguchi, T. & NEwMAN, W. A. A new and primitive barnacle (Cirripedia: Balanomorpha) from the North Fiji Basin abyssal hydrothermal field, and its evolutionary implications. (1990).
6. Guinot, D. & Segonzac, M. A review of the brachyuran deep-sea vent community of the western Pacific, with two new species of *Austinograea* Hessler & Martin, 1989 (Crustacea, Decapoda, Brachyura, Bythograeidae) from the Lau and North Fiji Back-Arc Basins. *Zoosystema* **40**, 1–36 (2018).
7. Hessler, R. R. & Martin, J. W. *Austinograea williamsi*, new genus, new species, a hydrothermal vent crab (Decapoda: Bythograeidae) from the Mariana Back-arc Basin, Western Pacific. *Journal of Crustacean Biology* **9**, 645–661 (1989).
8. SAINT LAURENT, M. de & MACPHERSON, E. Une nouvelle espèce du genre *Paralomis* White, 1856, des sources hydrothermales du Sud-ouest Pacifique (Crustacea, Decapoda, Lithodidae). *Zoosystema* **19**, 721–727 (1997).
9. Martin, J. W. & Hessler, R. R. *Chorocaris vandoverae*, a new genus and species of hydrothermal vent shrimp (Crustacea, Decapoda, Bresiliidae). *Contributions in Science* **417**, 1–11 (1990).
10. Zelnio, K. A. & Hourdez, S. A New Species of *Alvinocaris* (Crustacea: Decapoda: Caridea: Alvinocarididae) from hydrothermal vents at the Lau Basin, southwest Pacific, and a key to the species of Alvinocarididae. *Proceedings of the Biological Society of Washington* **122**, 52–71 (2009).
11. Cubelio, S. S., Tsuchida, S. & Watanabe, S. Vent associated *Munidopsis* (Decapoda: Anomura: Galatheidae) from Brothers Seamount, Kermadec arc, southwest Pacific, with description of one new species. *Journal of Crustacean Biology* **27**, 513–519 (2007).
12. Baba, K. & de Saint Laurent, M. Chirostylid and galatheid crustaceans (Decapoda: Anomura) from active thermal vent areas in the southwest Pacific. *Sci Mar* **56**, 321–332 (1992).
13. Chen, C., Xu, T., Fraussen, K. & Qiu, J.-W. Integrative taxonomy of enigmatic deep-sea true whelks in the sister-genera *Enigmaticolus* and *Thermosipho* (Gastropoda: Buccinidae). *Zool J Linn Soc* **193**, 230–240 (2021).
14. Ferrini, V. & Huang, S. Processed Gridded Near-Bottom Bathymetry Data from the Lau Back-arc Basin acquired with ROV ROPOS during R/V Falkor expedition FK160407 (2016). *Marine Geoscience Data System.* doi: 10.1594/IEDA/324649